

# A Simple Model for Complex Dynamical Transitions in Epidemics

David J. D. Earn,<sup>1,2\*</sup> Pejman Rohani,<sup>2</sup> Benjamin M. Bolker,<sup>3</sup>  
Bryan T. Grenfell<sup>2</sup>

Dramatic changes in patterns of epidemics have been observed throughout this century. For childhood infectious diseases such as measles, the major transitions are between regular cycles and irregular, possibly chaotic epidemics, and from regionally synchronized oscillations to complex, spatially incoherent epidemics. A simple model can explain both kinds of transitions as the consequences of changes in birth and vaccination rates. Measles is a natural ecological system that exhibits different dynamical transitions at different times and places, yet all of these transitions can be predicted as bifurcations of a single nonlinear model.

Apart from their public health importance, epidemics of childhood infections have provided valuable insights into theories of population dynamics (1–3). Before mass vaccination began in the 1960s, epidemics of measles exhibited both regular (annual, biennial, and triennial cycles) and irregular dynamics (3). In countries where mass immunization programs are now in place, measles epidemics have become more irregular as overall incidence has declined. In the United Kingdom, mass vaccination has also coincided with a sharp reduction in the geographical coherence of measles epidemics (4).

Mechanisms that sustain oscillations in the incidence of diseases such as measles are well known (1), but the causes of the transitions in patterns of epidemics are still poorly understood. Models that attempt to explain these transitions typically use the SEIR (Susceptible-Exposed-Infectious-Recovered) framework (5), using seasonal variation in transmission rate to mimic the aggregation of children in schools. Researchers using these models have emphasized endogenous dynamical explanations of transitions, based on chaos (3) or noise-driven shifts among coexisting stable cycles (6). These hypotheses suggest that it should be difficult or impossible to predict the timing and nature of specific transitions in measles dynamics. Here, we give an alternative explanation based on an exogenous factor—slow variation in the average rate of recruitment of new susceptibles—which allows us to predict measles transitions in large cities on the basis of published birth and vaccine uptake data.

It has been noted that annual cycles of measles epidemics occur in places where the birth rate is high (7). However, models normally take the average birth rate to be constant, implicitly ignoring the possibility that slow changes in this parameter could be a major driving force for dynamical transitions. We show that temporal changes in birth or vaccination rates can be associated with a variety of dynamical transitions in measles, and that all these transitions can be explained as bifurcations of a nonlinear dynamical system.

A very simple mathematical observation allows us to focus on a single parameter. For epidemic models that are not seasonally forced, it is an important standard result (8) that vaccination of a proportion  $p$  of the population effectively reduces the mean transmission rate  $\langle\beta\rangle$  by a factor  $1 - p$ . This correspondence also holds for the full nonlinear dynamics of seasonally forced epidemic models (9). We predict, therefore, that vaccination at level  $p$  will induce epidemic patterns identical to those in an unvaccinated population with mean transmission rate  $\langle\beta\rangle(1 - p)$ . In addition, we predict that changes in the birth rate  $v$  by a given factor should produce exactly the same dynamical transitions as changing  $\langle\beta\rangle$  by the same factor (9).

Thus, in general, changes in the susceptible recruitment rate  $v(1 - p)$  cause effective changes in the mean transmission rate  $\langle\beta\rangle$ . A single bifurcation diagram in  $\langle\beta\rangle$  therefore allows us to predict temporal transitions in measles dynamics, both before and after the start of mass immunization; all dynamical effects of changes in either birth or vaccination rates map onto a single axis.

The relation between recruitment rate and effective mean transmission rate, and the reduction of the problem to a single bifurcation diagram, do not depend in any way on the pattern of seasonality in transmission. However, for any given amplitude of seasonal variation, the

shape of the forcing function has a large effect on the dynamics (10). Consequently, for a given seasonal amplitude, the structure of the  $\langle\beta\rangle$  bifurcation diagram depends on the shape of the seasonal forcing function. Because the  $\langle\beta\rangle$  bifurcation diagram is central to predicting transitions, it is important to consider carefully both the amplitude and shape of the seasonal forcing function.

Traditionally, seasonality in transmission has been incorporated in the SEIR model as sinusoidal forcing (3), which is a poor representation of the true pattern of seasonality. We adopt a more realistic approach, setting transmission rates high during school terms and low otherwise [“term-time forcing,” originally proposed by Schenzle (2) as an element of a realistic age-structured model]. The amplitude of seasonality that can be estimated from data (11, 12) corresponds to term-time forcing, not sinusoidal forcing, so it is important to use the term-time forced SEIR model when comparing with data (13). It is not necessary to complicate the analysis by explicitly modeling age structure in the host population; we find (10) that the simple, term-time forced SEIR model behaves almost identically to recently favored age-structured models (2), indicating that the critical ingredient in measles models is a realistic seasonal forcing function rather than explicit modeling of heterogeneous transmission (10).

Figure 1 presents a bifurcation diagram for the term-time forced SEIR model, with fixed parameters chosen to correspond to measles. The control parameter (on the abscissa) is the mean transmission rate  $\langle\beta\rangle$ . The ordinate shows measles incidence on 1 January of each year, so annual cycles are represented by a single curve, biennial cycles by double curves, and so on. Different colors correspond to different stable solutions of the model, which attract different sets of initial conditions (basins of attraction).

For several values of the mean transmission rate  $\langle\beta\rangle$ , basins of attraction of the various attractors are shown above the bifurcation diagram in Fig. 1. Where multiple stable solutions coexist, stochasticity can induce complicated dynamics due to shifts among attractors (6). The upper panels of Fig. 1 show that the basins of coexisting attractors are more intermixed if  $\langle\beta\rangle$  is smaller, so we expect the effects of stochasticity to be greater for smaller  $\langle\beta\rangle$  (or, equivalently, when the effective  $\langle\beta\rangle$  is reduced by vaccination or a decrease in birth rate).

Figure 2 shows measles incidence in four representative large cities; major dynamical transitions are evident in each case. Superimposed on the time series, each panel shows births (in red). In the vaccine era, susceptible recruitment (light blue) is lower than births. Above the incidence data, horizontal lines indicate periods of annual, biennial, and more

<sup>1</sup>Department of Mathematics and Statistics, McMaster University, Hamilton, Ontario L8S 4K1, Canada.

<sup>2</sup>Department of Zoology, University of Cambridge, Downing Street, Cambridge CB2 3EJ, UK. <sup>3</sup>Zoology Department, University of Florida, Gainesville, FL 32611-8525, USA.

\*To whom correspondence should be addressed. E-mail: earn@math.mcmaster.ca

complex dynamics that are predicted (Fig. 1) on the basis of the observed exogenous variables (birth and vaccination rates). The horizontal lines in Fig. 2 are color-coded according to the corresponding attractors in Fig. 1.

London (Fig. 2A) experienced biennial cycles of measles epidemics from 1950 to 1968; the estimated mean transmission rate for this period ( $\langle \beta \rangle$ ) is  $\langle \beta \rangle \approx 1240$ , corresponding to a biennial attractor (dark blue, see Fig. 1). Before 1950, epidemics were roughly annual; over the same brief period the birth rate was much higher, which greatly increased the effective mean transmission rate, allowing attraction to an annual cycle (green, far right of Fig. 1). After 1968, recruitment rates steadily decreased because of mass vaccination (for example, when vaccine uptake reached 60%, the effective mean transmission rate was reduced to  $\langle \beta \rangle \approx 500$ ); this brought the system into the parameter region where there are multiple coexisting attractors with extremely intermixed basins. Stochastic effects do appear to cause frequent random jumps between these attractors (6) [as we have confirmed with Monte Carlo simulations (14)], providing an explanation for the irregular epidemics in the vaccine era. Alternatively, or in addition, irregular dynamics in this region may arise from stochastic interactions with a chaotic repellor (15, 16). Spectral analysis of the data in the vaccine era shows two major peaks, at periods of 1 year and 2 to 3 years; spectral analysis reveals similar peaks in our Monte Carlo simulations (14).

In Liverpool (Fig. 2B) the birth rate was much higher than the mean in England and Wales throughout the post-war period until 1968 (12) (the birth rate in Liverpool is drawn as a dotted red line in Fig. 2A as well, for comparison with the birth rate in London). This explains the roughly annual cycle of measles epidemics over the same period. After 1968, the combination of vaccination and a lower birth rate brought Liverpool, like London, into the regime where irregular dynamics are predicted.

Birth rates in the United States were relatively low during the Great Depression. Throughout this period, measles epidemics were irregular in New York and Baltimore (Fig. 2, C and D), consistent with stochastic switching between densely intermixed attractors or a chaotic repellor. After World War II, birth rates rose dramatically, pulling the system out of the regime with irregular dynamics. In New York, the birth rate quickly reached a plateau, apparently fixing the system on the biennial attractor. In Baltimore, the birth rate continued to rise, eventually enough to bring the effective  $\langle \beta \rangle$  into the region of Fig. 1 where either biennial or annual cycles are possible (far right of Fig. 1).

Developing countries provide a final example. There, birth rates over the periods shown in Fig. 2 were far higher than those in

Britain or the United States (7). The demographic parameters for developing countries during this period lie beyond the right-hand limit of the bifurcation diagram in Fig. 1. We therefore expect strictly annual prevaccine measles dynamics in these countries—again consistent with time series data (7)—and the possibility of more complex dynamics with increasing vaccination levels (moving the system to the left in Fig. 1).

In addition to the transitions in temporal dynamics, Fig. 1 may explain the desynchronization of measles epidemics after the introduction of mass vaccination in England and Wales (4). After the start of mass vaccination, all cities entered the regime in which multiple stable cycles may coexist. To maintain synchrony under such circumstances, different cities must do more than remain in phase; they must lock onto the same attractor at all times. We expect less and less synchrony as vaccination levels increase because the basins of coexisting attractors will become more densely intermixed (Fig. 1, upper panels), increasing the probability that stochasticity will cause shifts among attractors. In addition, mass vaccination may increase the effective magnitude of demographic stochasticity, because the pool of susceptible individuals is greatly reduced.

The bifurcation diagram in Fig. 1 is plotted for a particular seasonal amplitude, but the qualitative conclusions of the above discussion are similar for a wide range of amplitudes. For higher seasonality, the region with many attractors contains chaotic attractors as well. Such high seasonal amplitudes would not change our conclusion that measles dynamics will be irregular in this region. For lower seasonality, many of the attractor sequences cease to exist or end at higher  $\langle \beta \rangle$ , but the “ghosts of departed attractors” still influence the dynamics for low  $\langle \beta \rangle$ : There are extremely long and erratic transient dynamics (17) in this region. Again, this supports our prediction of irregularity, so we would expect the same qualitative dynamical picture to emerge in places that have significantly higher or lower externally imposed seasonality.

Ecologists often test theoretical models by manipulating the conditions of their study populations so as to stimulate dynamical changes (18). For measles and other parasitic infections, many such manipulations have been achieved indirectly (through changes in birth and vaccination rates) and monitored in

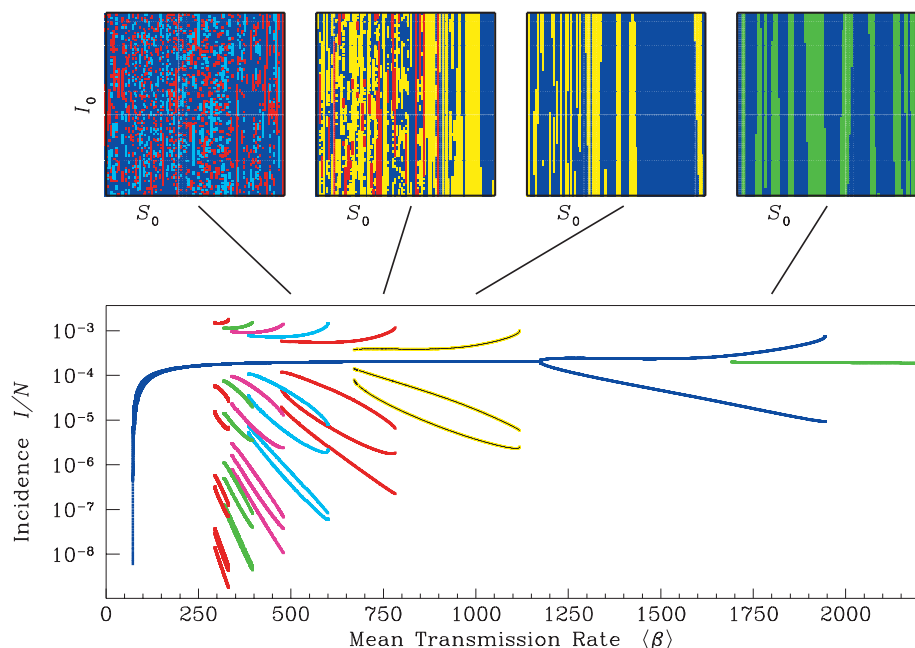


**Fig. 1.** The main panel is the bifurcation diagram for the term-time forced SEIR model, showing incidence on 1 January, normalized by (constant) population size; the control parameter is the mean transmission rate  $\langle \beta \rangle$ . The fixed parameter values are  $\gamma^{-1} = 5$  days,  $\sigma^{-1} = 8$  days,  $\mu = v/N = 0.02$  year<sup>-1</sup>, seasonal amplitude 0.25 [see (5) and (13) for the meaning of these parameters]. Each attractor is identified with a different color. For sufficiently high  $\langle \beta \rangle$ , there is a unique (annual) attractor. As  $\langle \beta \rangle$  is reduced, biennial, 3-, 4-, 5-, 6-, 7-, and 8-year cycles all occur, before all but the annual attractor are extinguished. The term-time forcing function used to produce this figure corresponds to school terms in England and Wales. In the United States, the summer holiday is longer; this does not affect the structure of the bifurcation diagram, but with a longer summer holiday each of the various bifurcations occurs at lower  $\langle \beta \rangle$  (10). Above the bifurcation diagram, basins of attraction (initial susceptibles,  $0 < S_0/N < 0.1$ , versus initial infectives,  $0 < I_0/N < 0.0001$ , with  $E_0/N = 0.0001$ ) are shown for the various attractors at four particular values of  $\langle \beta \rangle$ . Figure 2 identifies regions of this diagram that correspond to the dynamics observed at various times and places.

great detail by the medical community. These “natural experiments” vary sufficiently in both space and time that we have been able to use them to explore the nonlinear dynamics of measles epidemics, mapping observed dynamics onto the bifurcation cascade that results from changes in effective transmission rate. Further opportunities to explore nonlinear ecological processes abound in infectious disease data.

A very simple analysis of the SEIR model (9) has enabled us to relate dramatic shifts in measles dynamics to changes in the susceptible recruitment rate in the host population, and to propose simple explanations of observed dynamical transitions in individual cities and in the pattern of synchrony among cities. An important implication is that it may be possible to design vaccination programs that induce desirable dynamical transitions [such as greater spatial synchrony, which may increase the probability of global eradication (14, 19)].

Recognizing the low impact of contact

heterogeneity among age groups (2) has highlighted the importance of seasonal variation in transmission (which stimulates oscillations in incidence) and long-term trends in birth and vaccination rates (which drive dynamical transitions). This simplification (10) also implies a major analytical and computational benefit for future investigations of the spatio-temporal dynamics of measles.

Our results reinforce the conviction of many empiricists that exogenous effects are critically important, but indicate that these effects should be studied simultaneously with nonlinear feedbacks in ecological and epidemiological systems. In the past, epidemic models have addressed these two phenomena separately, either by tracking responses of equilibria or nearly linear dynamics to exogenous changes (1) or by considering nonlinear dynamics in isolated systems with constant parameters (3). We have considered the effects of slowly changing exogenous forces on a nonlinear system and have successfully predicted the complex patterns of measles

incidence. The general lesson for ecologists, epidemiologists, and dynamicists is that complex dynamical transitions in ecological systems may often have simple underlying exogenous explanations.

#### References and Notes

1. M. S. Bartlett, *J. R. Stat. Soc. A* **120**, 48 (1957); R. M. Anderson and R. M. May, *Infectious Diseases of Humans: Dynamics and Control* (Oxford Univ. Press, Oxford, 1991); B. T. Grenfell, *J. R. Stat. Soc. B* **54**, 383 (1992); B. Grenfell and J. Harwood, *Trends Ecol. Evol.* **12**, 395 (1997); S. A. Levin, B. Grenfell, A. Hastings, A. S. Perelson, *Science* **275**, 334 (1997); C. Zimmer, *Science* **284**, 83 (1999).
2. D. Schenzle, *IMA J. Math. Appl. Med. Biol.* **1**, 169 (1984); B. M. Bolker and B. T. Grenfell, *Proc. R. Soc. London Ser. B* **251**, 75 (1993); D. Mollison and S. Ud Din, *Math. Biosci.* **117**, 155 (1993); N. M. Ferguson, R. M. May, R. M. Anderson, in *Spatial Ecology*, D. Tilman and P. Kareiva, Eds. vol. 30 of *Monographs in Population Biology* (Princeton Univ. Press, Princeton, NJ, 1997), pp. 137–157.
3. W. London and J. A. Yorke, *Am. J. Epidemiol.* **98**, 453 (1973); W. M. Schaffer, *IMA J. Math. Appl. Med. Biol.* **2**, 221 (1985); W. Schaffer and M. Kot, *J. Theor. Biol.* **112**, 403 (1985); L. F. Olsen, G. L. Truty, W. M. Schaffer, *Theor. Pop. Biol.* **33**, 344 (1988); L. F. Olsen and W. M. Schaffer, *Science* **249**, 499 (1990); W. Schaffer, B. Kendall, C. Tidd, L. Olsen, *IMA J. Math. Appl. Med. Biol.* **10**, 227 (1993); R. Engbert and F. R. Drepper, in *Predictability and Nonlinear Modelling in Natural Sciences and Economics*, J. Gasman and G. van Straten, Eds. (Kluwer, Dordrecht, Netherlands, 1994), pp. 204–215; P. Glendinning and L. P. Perry, *J. Math. Biol.* **35**, 359 (1997); S. P. Ellner et al., *Am. Nat.* **151**, 425 (1998).
4. B. M. Bolker and B. T. Grenfell, *Proc. Natl. Acad. Sci. U.S.A.* **93**, 12648 (1996).
5. The dynamical equations for the SEIR model (1) are
 
$$\frac{dS}{dt} = \nu - (\beta I + \mu)S \quad (1a)$$

$$\frac{dE}{dt} = \beta S - (\sigma + \mu)E \quad (1b)$$

$$\frac{dI}{dt} = \sigma E - (\gamma + \mu)I \quad (1c)$$

$$\frac{dR}{dt} = \gamma I - \mu R \quad (1d)$$
6. I. B. Schwartz and H. Smith, *J. Math. Biol.* **18**, 233 (1983); I. B. Schwartz, *J. Math. Biol.* **21**, 347 (1985); J. L. Aron, *Theor. Pop. Biol.* **38**, 58 (1990).
7. A. McLean and R. Anderson, *Epidemiol. Infect.* **100**, 111 (1988); *Epidemiol. Infect.* **100**, 419 (1988); B. Grenfell, A. Kleczkowski, S. Ellner, B. Bolker, *Philos. Trans. R. Soc. London Ser. A* **348**, 515 (1994).
8. R. M. May, in *Biomathematics*, T. Hallam and S. Levin, Eds. (Springer-Verlag, Berlin, 1986), vol. 17, pp. 405–442.
9. If a proportion  $\rho$  of newborns is vaccinated then Eqs. 1a and 1d become
 
$$\frac{dS}{dt} = \nu(1 - \rho) - (\beta I + \mu)S$$

$$\frac{dR}{dt} = \nu\rho + \gamma I - \mu R$$

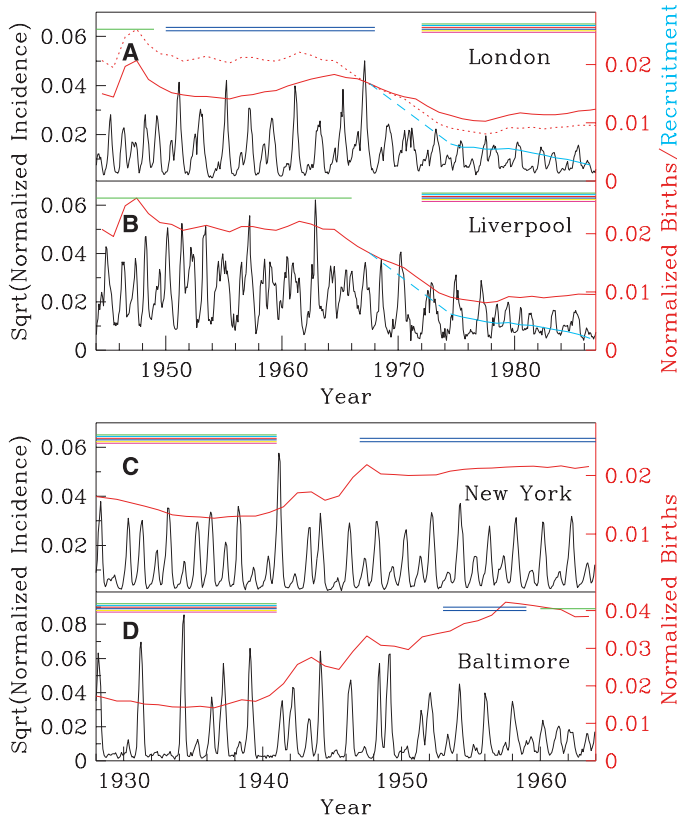


**Fig. 2.** Measles dynamics in four large cities. (A) London, (B) Liverpool, (C) New York, and (D) Baltimore. In each panel, the black time series shows the square root of measles incidence normalized by the population size in 1960 (5) (the data are 4-weekly in the United Kingdom and monthly in the United States). The red curve shows annual births normalized by the population size in 1960 (5). In (A) and (B), the light blue curve shows (normalized) annual susceptible recruitment (which is lower than the birth rate in the vaccine era). Together with the mean transmission rate ( $\beta$ ), the recruitment rate determines the nature of the dynamics, as discussed in the main text and (9) (effects of changes in birth rate will be delayed by initial maternally acquired immunity and the age of school entry). The vertical scale for Baltimore is higher because reporting rates were twice as high [see London and Yorke (3)]. Note that the American data cover an earlier period than the English data; perhaps because of increases in mobility with time (as well as differences in population density), estimated values of  $\langle \beta \rangle$  are significantly lower for the American cities (20). This (and the length of the summer holiday; see legend to Fig. 1) must be borne in mind when comparing measles incidence data with various regions of Fig. 1. The colored lines at the top of each panel correspond to the region of the bifurcation diagram in Fig. 1 that applies to each section of the measles time series. Many colored lines together indicate the region of Fig. 1 containing many coexisting attractors with intermixed basins. Two horizontal blue lines indicate the biennial attractor in Fig. 1, while the single green line indicates the annual attractor that exists for high transmission rates. Gaps, where no region of Fig. 1 is indicated, correspond to transient periods when the recruitment rate changed relatively rapidly.

## REPORTS

- and the other SEIR equations are unchanged. Now consider a simple change of variables:  $S = S'(1 - p)$ ,  $E = E'(1 - p)$ ,  $I = I'(1 - p)$ , and  $R = R'(1 - p) + (\nu/\mu)p$ . The dynamical equations for the primed variables are exactly the SEIR equations without vaccination, i.e., Eqs. 1, except that the transmission rate  $\beta$  is replaced everywhere by  $\beta(1 - p)$ . Thus, except for an overall reduction in the number of cases, when a proportion of a population is vaccinated the dynamics are identical to those of an unvaccinated SEIR system with a smaller mean transmission rate,  $\langle\beta\rangle \rightarrow \langle\beta\rangle(1 - p)$ . Because birth rate  $\nu$  enters the  $dS/dt$  equation in exactly the same place as vaccination, a similar argument applies to changes in birth rate. A change in birth rate from  $\nu$  to  $\nu'$  is dynamically equivalent to a change from  $\langle\beta\rangle$  to  $\langle\beta\rangle(\nu'/\nu)$ . This is why we can predict the character of the population dynamics of measles (or other infections) after vaccination or birth rate changes, and explain a wide variety of data with a single diagram (Fig. 1).
10. D. J. D. Earn, B. M. Bolker, P. Rohani, B. T. Grenfell, in preparation.
  11. P. E. Fine and J. A. Clarkson, *Int. J. Epidemiol.* **11**, 5 (1982).
  12. B. F. Finkenstädt and B. T. Grenfell, *Proc. R. Soc. London Ser. B* **265**, 211 (1998).
  13. Good fits to measles incidence times series can be

- obtained with the SEIR model only if term-time forcing is used. However, in (10) we show that the sequence of bifurcations in the term-time forced SEIR model is reproduced by the sinusoidally forced SEIR model (at much lower forcing amplitude). A relevant bifurcation diagram can therefore be generated using sinusoidal forcing, though only if the appropriate amplitude is determined, which is a somewhat subtle procedure (10). Most previous discussions of measles dynamics have assumed sinusoidal seasonal forcing with an amplitude of 0.28, which yields a chaotic attractor (3); this level of forcing is about three times higher than it should be. A term-time forcing amplitude of 0.25 (used in Fig. 1) corresponds to a sinusoidal forcing amplitude of roughly 0.08 (10).
14. P. Rohani, D. J. D. Earn, B. T. Grenfell, *Science* **286**, 968 (1999).
  15. D. A. Rand and H. B. Wilson, *Proc. R. Soc. London Ser. B* **246**, 179 (1991).
  16. Because the seasonal amplitude cannot be measured precisely (and longer time series are not available) we will probably never be certain whether periods of irregularity in measles time series arise from stochastic hopping between coexisting attractors or stochastic interactions with (possibly chaotic) repellors. However, it seems that irregular behavior must be induced to some extent by noise, i.e., the source of

irregularity cannot be a chaotic attractor. Seasonal amplitudes above the minimum required for a chaotic attractor to be reached appear to be ruled out by the data (10, 13).

17. A. Hastings and K. Higgins, *Science* **263**, 1133 (1994).
18. R. F. Costantino, R. A. Desharnais, J. M. Cushing, B. Dennis, *Science* **275**, 389 (1996); M. Holyoak and S. P. Lawler, *J. Anim. Ecol.* **65**, 640 (1996); P. J. Hudson, A. P. Dobson, D. Newborn, *Science* **282**, 2256 (1998); P. Turchin, A. D. Taylor, J. D. Reeve, *Science* **285**, 1068 (1999).
19. D. J. D. Earn, P. Rohani, B. T. Grenfell, *Proc. R. Soc. London Ser. B* **265**, 7 (1998).
20. R. M. Anderson, Ed., *The Population Dynamics of Infectious Diseases: Theory and Applications* Chapman and Hall, London, (1982).
21. We thank S. Balshine, O. Bjørnstad, B. F. Finkenstädt, R. A. Johnstone, S. A. Levin, D. A. Price, and the anonymous referees for helpful comments. Supported by a Wellcome Trust postdoctoral research fellowship in mathematical biology (D.J.D.E.), a Natural Environment Research Council postdoctoral research fellowship and a Royal Society University Research Fellowship (P. R.), and the Wellcome Trust (B.T.G.).

24 September 1999; accepted 26 November 1999

Science ~~ONLINE~~

# Take a hike!

In our Enhanced Perspectives, we navigate the virtual forest for you. Each week, one Perspective from *Science's Compass* links readers to the best related Web-based content:

- research databases
- tutorials
- glossaries
- abstracts
- other online material

Take your virtual hike at [www.sciencemag.org/misc/e-perspectives.shtml](http://www.sciencemag.org/misc/e-perspectives.shtml)